HENRY
Hydraulic Engineering Repository

Ein Service der Bundesanstalt für Wasserbau

Conference Paper, Published Version

Fonias, E.; Breugem, W. Alexander; Wang, Li; Bolle, Annelies; Kolokythas, Gerasimos; De Maerschalck, B.

Implementation of cross-shore processes in GAIA

Zur Verfügung gestellt in Kooperation mit/Provided in Cooperation with:
TELEMAC-MASCARET Core Group

Verfügbar unter/Available at: https://hdl.handle.net/20.500.11970/108303

Vorgeschlagene Zitierweise/Suggested citation:
Fonias, E.; Breugem, W. Alexander; Wang, Li; Bolle, Annelies; Kolokythas, Gerasimos; De Maerschalck, B. (2021): Implementation of cross-shore processes in GAIA. In: Breugem, W. Alexander; Frederickx, Lesley; Koutrouveli, Theofano; Chu, Kai; Kulkarni, Rohit; Decrop, Boudewijn (Hg.): Proceedings of the papers submitted to the 2020 TELEMAC-MASCARET User Conference October 2021. Antwerp: International Marine and Dredging Consultants (IMDC). S. 138-143.

Standardnutzungsbedingungen/Terms of Use:

Die Dokumente in HENRY stehen unter der Creative Commons Lizenz CC BY 4.0, sofern keine abweichenden Nutzungsbedingungen getroffen wurden. Damit ist sowohl die kommerzielle Nutzung als auch das Teilen, die Weiterbearbeitung und Speicherung erlaubt. Das Verwenden und das Bearbeiten stehen unter der Bedingung der Namensnennung. Im Einzelfall kann eine restriktivere Lizenz gelten; dann gelten abweichend von den obigen Nutzungsbedingungen die in der dort genannten Lizenz gewährten Nutzungsrechte.

Documents in HENRY are made available under the Creative Commons License CC BY 4.0, if no other license is applicable. Under CC BY 4.0 commercial use and sharing, remixing, transforming, and building upon the material of the work is permitted. In some cases a different, more restrictive license may apply; if applicable the terms of the restrictive license will be binding.

Verwertungsrechte: Alle Rechte vorbehalten

Implementation of cross-shore processes in GAIA

E Fonias[1,2], WA Breugem[1], L Wang[1,2], A Bolle[1]
[1] International Marine and Dredging Consultants
Antwerp, Belgium
efstratios.fonias@imdc.be

G Kolokythas[2], B De Maerschalck[2]
[2] Flanders Hydraulics Research
Antwerp, Belgium

***Abstract*—In the present paper, a first attempt is presented to add cross-shore sediment transport processes within the module GAIA of TELEMAC-MASCARET. Consideration of Stokes drift, return flow and wave non-linearity mechanisms was implemented. A comparison was performed with a laboratory experiment, showing promising results.**

I. INTRODUCTION

Cross-shore transport processes are quite complex phenomena because they depend on the balance between wave effects and mean currents that can cause either onshore or offshore transport. Thus, cross-shore sediment transport gradients can be significant and cause morphological changes that can be intense spatially and temporally, particularly in storm events [9]. For example, convergence in cross-shore sediment transport rates result in the formation of bars, observed in the vicinity of the breaking zone. As shown by [5], nearshore bars move offshore within storm periods, whereas in cases of mild waves they propagate onshore. In particular when the ratio of the significant wave height to water depth above crest is higher than 0.6 the bars move offshore and when it is smaller than 0.3 they move onshore.

Accurate computation of cross-shore sediment transport in the nearshore is a rather challenging procedure. Several mechanisms with different effect and intensity are in motion balancing onshore and offshore transport processes. Onshore transport mechanisms include Stokes drift, streaming and wave non-linearity (skewness and asymmetry). Offshore processes include return flow, gravity, and long waves.

Stokes drift is causing net mass transport towards the coast. Due to continuity, a return flow or *undertow*, is formed. Streaming is a steady current induced by surface waves close to the boundary layer and contributes to onshore sediment transport [17] (see Figure 1).

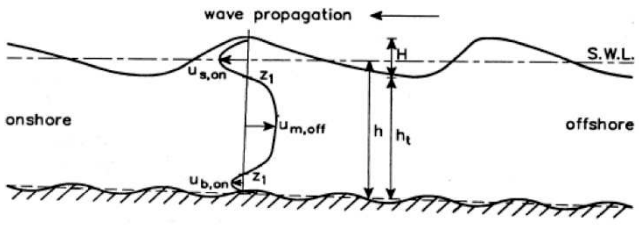

Figure 1 – Time averaged velocity profile [17] showing from top to bottom: Stokes drift (u_s), return flow (u_m) and streaming (u_b). From [17]

Wave non-linearity (skewness and asymmetry) contributes to the onshore transport by higher waves but with shorter crests than troughs (skewness) and a steeper wave front than the tail of the crest (asymmetry). Skewness is often considered as the dominant mechanism for onshore transport. However, this argument is still under debate and depends on sediment characteristics [8], [4]. Wave roller quantifies the energy dissipation due to wave breaking that occurs within an amount of time. Due to this temporal delay, the location of wave breaking and sediment concentration moves closer to the coast and this results in offshore transport due to the return flow from these rollers. Finally, 3D effects are important to explain cross-shore transport phenomena, as longshore transport is combined with cross-shore transport. For instance, 3D effects such as shear waves, edge waves and rip currents are important to reproduce coastal bars formation [1], [21].

Long waves result in offshore transport. Their contribution is smaller than wave non-linearity in sediment transport [6]. Long waves or surf beat result in dune erosion. In those cases, long waves and return flow have a stronger effect than wave non-linearity [15].

Gravity stabilizes sediment and smooths out morphological features especially in bars. It tends, on average, to transport sediment offshore due to foreshore slope.

In addition, vertical pressure gradients result in infiltration and exfiltration in the seabed and contribute to both onshore and offshore transport [7]. During exfiltration, those pressure gradients result in destabilized sediment and increasing near-bed concentrations. At the same time, the boundary layer thickness increases as turbulent eddies are released, which results in lower near bed velocities. Those mechanisms are reversed in case of infiltration.

Turbulence, fall velocity, bed forms, wind stress, wave roller and 3D effects are mechanisms that could result in either onshore or offshore transport.

Turbulence is the basic reason for the different transport behavior in shoaling zone and in surf zone. In the shoaling zone, there are high sediment concentrations in the near bed region, which are transported onshore. In the surf zone, turbulence occurs due to wave breaking, which results in sediment concentrations in the full water column and thus return flow becomes dominant resulting in offshore transport [6]. Based on the magnitude of the fall velocity, the suspended sediment particles can be caught in the crest or the trough of the wave, which determines whether they will be moving onshore or offshore [23].

Bed forms can affect the flow through secondary mechanisms such as changes in bed roughness [1], and depend on the intensity of local flow conditions. That is the reason why spatial variability of bed forms is evident on cross-shore profiles. Wind stress can impose a more intense flow by means of a shear stress on water surface, especially during storm events. This is compensated by a

bottom flow towards the opposite direction in the nearshore. When wind stress is combined with a Coriolis force, this generates upwelling and onshore transport or downwelling and offshore transport [14]. Those mechanisms will not be investigated in the present paper.

TABLE 1– RELATIVE IMPORTANCE OF PROCESSES FOR ONSHORE TRANSPORT, OFFSHORE TRANSPORT AND BAR BEHAVIOR [18]. THE "+" SIGN INDICATES HIGH IMPORTANCE OF THE MECHANISM, THE "-" LOW , AND THE "=" BALANCED EFFECT. MORE INTENSE CONTRIBUTIONS ARE INDICATED BY DOUBLE PLUS OR MINUS SIGNS.

Process	Onshore transport	Offshore transport	Bar behavior
Stokes drift	-		-
Return flow		++	++
Streaming	-		-
Wave asymetry	+		+
Wave skewness	++		++
In- and Exfiltration	--	--	--
Gravity		=	+
Turbulence	=	=	+
Wind stress	-	-	-
Fall velocity	--	-	--
Bed forms	-	-	=
Long waves	-	++	++
Wave roller			+
3D effects			- → ++

The relative importance of each process determines whether the sediment is transported onshore or offshore and depends on hydrodynamic conditions which are milder in summer and more intense in winter. The relative importance is shown in Table 1 for onshore transport, offshore transport and bar behavior [18]. The "+" sign indicates high importance of the mechanism, the "-" low , and the "=" balanced effect. More intense contributions are indicated by double plus or minus signs.

Several of the processes that are important for offshore and onshore transport have not yet been included in the TELEMAC-MASCARET suite. The present work is focused on the implementation of the Stokes drift, return flow, and wave non-linearity (both due to wave asymmetry and wave skewness), inspired by the available physical parametrizations in XBeach. The implementation of surface rollers was discussed in a separate paper [24], whereas the effect of long waves is also significant but it has not been implemented in the present work. The developments presented here were implemented in the framework of developing a morphological model of the Belgian Coast: the Scaldis-Coast model [11]. It shows the first step in implementing cross-shore processes in TELEMAC-MASCARET. The new implementations are tested for a laboratory test case coupling TELEMAC-2D, TOMAWAC and GAIA presented here, and the patterns in the bed morphology are discussed.

II. MATHEMATICAL MODEL AND CODE IMPLEMENTATION

A. General features

The GAIA modification for considering the cross-shore sediment transport processes include modification of the depth averaged flow velocities that will be used for computation of suspended sediment transport using the advection-diffusion equation:

$$\frac{\partial hC}{\partial t}+\frac{\partial hU^E C}{\partial x}+\frac{\partial hV^E C}{\partial y}=\frac{\partial}{\partial x}\left(h\varepsilon_s\frac{\partial C}{\partial x}\right)+\frac{\partial}{\partial y}\left(h\varepsilon_s\frac{\partial C}{\partial y}\right)+E-D \quad (1)$$

where C is the depth-averaged concentration, t is time, x and y are the two horizontal dimensions of the numerical domain, U^E,V^E are the Eulerian velocities , h is the water depth, ε_s is the eddy viscosity, and E and D are the non-cohesive erosion and deposition, respectively.

The additional velocity components accounting for cross-shore transport are based on formulations implemented in XBeach [12] and they are explained in detail in the following sections. This is achieved within the newly added subroutine `GAIA_CROSS_SHORE`.

In our approach, the generalized Lagrangian mean velocities U^L,V^L are given as:

$$U^L = U^E + U^S \ , \ V^L = V^E + V^S \quad (2)$$

where U^S,V^S are the velocities due to Stokes drift. The sediment transport needs to be calculated using the Eulerian velocity in the advection-diffusion equation. However, the velocities calculated by TELEMAC-2D are the Lagrangian velocities U^L,V^L. Therefore, one can take the effect of Stokes drift and the return current generated by the Stokes drift into account using:

$$U^E = U^L - U^S \ , \ V^E = V^L - V^S \quad (3)$$

In case we have waves moving towards the coast in a stationary situation, we have U^L=0 (no net flow of water towards the coast, and therefore U^E=-U^S, showing that the return current (U^E) is opposite to the Stokes drift [10].

The depth averaged flow velocities used for accounting for cross-shore sediment transport have the form of:

$$U^{tot} = U^L + \sin\theta\,(U_{NL} - U_{ST}) \quad (4)$$
$$V^{tot} = V^L + \cos\theta\,(U_{NL} - U_{ST})$$

The terms in these equations due to Stokes drift (U_{ST}, and wave non-linearity U_{NL}) are explained in the next sections and θ is the wave direction (TOMAWAC convention, i.e. 0 degrees for waves going to the North).

B. Stokes drift and Return flow

The Stokes drift occurs in the nearshore in the upper part of the water column (see Figure 1), because the motion of water particles do exhibits a perfectly circular track. As the horizontal orbital velocity increases with the distance from seabed [16], it leads to lower seaward velocities under the wave trough than the shoreward velocities under the wave crest.

This velocity difference has a magnitude of the order of 0.1 m/s in shallow water. The Stokes drift is taken into account by adding an extra velocity with magnitude U_{ST} and components U^S,V^S, based on the expression [12]:

$$U_{ST} = {}^{E_w}/_{\rho hc} \quad (5)$$
$$U^s = U_{ST}\sin\theta \quad , \quad V^s = U_{ST}\cos\theta$$

where U^s and V^s are the velocity components due to the Stokes drift [19], E^w is the wave-group varying short wave energy computed by:

$$E^w = {}^{\rho g H_s^2}/_{16} \quad (6)$$

In the above expression ρ is the water density, c is the phase velocity, g is the gravitational acceleration and H_s is the significant wave height.

C. Wave non-linearity

The wave non-linearity consists of wave skewness and wave asymmetry.

The wave skewness (*Sk*) indicates that wave crests are higher and shorter in duration than the troughs. The shoreward velocity under the crest is higher than the seaward velocity under the wave trough (skewness). Even though the mean orbital velocity is zero, the resulting mean bed shear stress is directed onshore.

Wave asymmetry (*As*) refers to the higher acceleration of the wave front compared to the wave tail. Phase lag effects (asymmetry) between maximum velocity and flow reversal has effect on sediment stirring [8]. Finally, horizontal pressure gradients can result in plug flow, or loosening up of sediment blocks from the bed. This phenomenon is more intense for asymmetric waves [10] resulting in onshore transport.

The contribution of wave non-linearity is calculated by means of an extra velocity with magnitude U_{NL} and components U^a,V^a:

$$U_{NL} = (f_{Sk}Sk - f_{As}As)u_{rms} \quad (7)$$
$$U^a = U_{NL}\sin\theta \quad , \quad V^a = U_{NL}\cos\theta$$

where f_{Sk} and f_{As} are calibration factors with values from 0 to 1.0 and a recommended value of 0.1, u_{rms} is the root-mean square velocity computed as:

$$u_{rms} = U_w\sqrt{2} \quad (8)$$

and U_w is the orbital velocity, calculated in TOMAWAC. Then, the skewness and asymmetry can be computed using the Boltzmann sigmoid through the expressions [12]:

$$Sk = B\cos\psi \quad , \quad As = B\sin\psi$$
$$\psi = -90 + 90\tanh\left({}^{p_5}/_{Ur^{p_6}}\right) \quad (9)$$
$$B = p_1 + {}^{(p_2 - p_1)}\Big/\left(1 + exp\,\tfrac{p_3 - logUr}{p_4}\right)$$

where *Ur* is the Ursell number computed by:

$$Ur = {}^3/_4 \cdot \left[{}^{0.5H_s k}/_{(kh)^3}\right] \quad (10)$$

and k is the wave number. $p_{1:6}$ are parametrization factors based on field observations [3]. In the present work we considered the mean values as:

$$p_1 = 0.000\ ,\ p_2 = 0.875\ ,\ p_3 = 0.471 \quad (11)$$
$$p_4 = 0.297\ ,\ p_5 = 0.815\ ,\ p_6 = 0.672$$

Variables including local orbital velocity, significant wave height, water depth and wave direction are communicated directly from TOMAWAC, whereas the wave celerity is calculated form the wave period and the wave number, which is computed using the subroutine `WNSCOU` using the local water depth and the wave period from TOMAWAC.

D. Bed slope effect

The bed slope can influence sediment transport, favouring sediment transport down the slope. This can result in different transport rate in terms of magnitude and/or direction. Inspired by the implementation in XBeach [12], the effect of the bed slope is parametrized by changing the sediment transport velocity shown in equation (4), using the following expression (with β as calibration coefficient) :

$$U^{tot} = U^{tot}\left(1 - \beta\frac{\partial\eta}{\partial x}\right) \quad (12)$$
$$V^{tot} = V^{tot}\left(1 - \beta\frac{\partial\eta}{\partial y}\right)$$

E. An updated advection scheme

The application of the above modifications leads to a sediment transport velocity field, that is not divergence free. The residual distribution schemes in TELEMAC were designed for the computation of advection for flow fields calculated in TELEMAC, that exactly conserve the water mass. Adding extra velocity components to schematize the cross-shore components, the velocity field used to advect the sediment is not mass conservative anymore. The added effects are merely parametrization that did not consider any mass balance in their derivation.

In order to have mass conservation for cross-shore transport, an updated advection scheme was implemented, based on the NERD scheme (`SCHEME FOR ADVECTION OF TRACERS = 13 or 14`) and for the ERIA scheme (`SCHEME FOR ADVECTION OF TRACERS = 15`). This scheme was specifically developed in order to perform well for flow fields that are not mass-conservative.

In deriving this scheme, we start from the continuity equation in the conservative form:

$$\frac{\partial hC}{\partial t} + \frac{\partial hCU}{\partial x} + \frac{\partial hCV}{\partial y} = 0$$

It can clearly be seen, that the product hC is the quantity that needs to be conserved. Therefore, we perform advection on the sediment volume ξ=hC. Using this substitution, and applying the product rule on the spatial derivatives we get the non-conservative form of the advection equation, (because all TELEMAC residual distribution schemes are based on the non-conservative form):

$$\frac{\partial\xi}{\partial t} + U\frac{\partial\,\xi}{\partial x} + V\frac{\partial\,\xi}{\partial y} = -\xi\left(\frac{\partial U}{\partial X} + \frac{\partial V}{\partial Y}\right)$$

This shows the following consequences for the updated advection scheme:

- The sediment volume in the time derivative is discretised by:

$$\frac{c^{n+1}H^{n+1} - c^{n}H^{n}}{\Delta t}$$

Hence, in order to get the sediment volume the concentration is multiplied by the water depth at time step *n*. To return to the depth-averaged concentration, the depth-integrated concentration needs to be divided by the water depth at time step *n+1* after the calculation of the advection.

- The sediment volume needs to be advected by the depth-averaged velocity field (in TELEMAC given by 'VGRADP', rather than by the depth integrated fluxes that are originally used in the NERD and ERIA schemes (variable; ' HUGRADP'))
- An extra source term is needed to take into account the fact that the velocity field is not divergence-free (this is the term on the right hand-side of the equation). This source term is added to the advection scheme. It is discretised implicitly in case the right hand side of the equation is negative (i.e. when it is a sink term) and explicitly when it is positive (i.e. when it is a source).

II. VALIDATION OF THE ADVECTION SCHEMES

A. *Constant velocity in increasing water depth*

The first validation case concerns a channel flow case of 2500 m length, with constant flow of 0.5 m/s in a channel with a uniformly increasing water depth. The spatial grid size is equal to 50 m and the time step equal to 10 s. The ERIA scheme has been used for this simulation. In this case the water depth is linearly increasing as it can be seen in Figure 2. The resulting solution of sediment concentration (solid line) is compared to the analytical solution (dashed line) derived using the method of characteristics. The results compare reasonably well, but the used advection scheme shows a substantial amount of numerical diffusion. A check of the mass balance showed that the mass of the advected tracer was conserved in this test case (not shown).

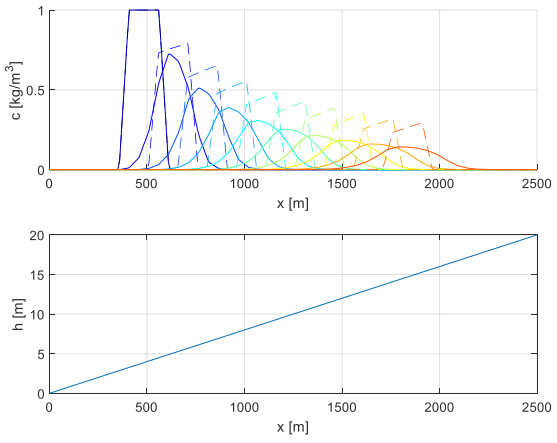

Figure 2 – Upper figure: temporal variation of suspended sediment concentration calculated using the updated ERIA scheme (solid lines) and comparison with the analytical solution (dashed lines). Lower figure: increase of the water depth along the channel.

B. *Accelerating flow*

The second validation case concerns a flow on the same channel where this time the water depth is remaining constant and the velocity increases from 0 m/s to 0.4 m/s. The ERIA scheme is used in this case as well. In Figure 3 the temporal variation of suspended sediment concentration along the length of the trench has been shown for the original ERIA scheme and for the modified ERIA scheme. In this case, the derivation of an analytical solution was not possible. In Figure 4, the mass is plotted for the original and modified schemes proving that the mass is conserved for the modified ERIA advection scheme, whereas in the original ERIA scheme, there is an issue with the mass balance.

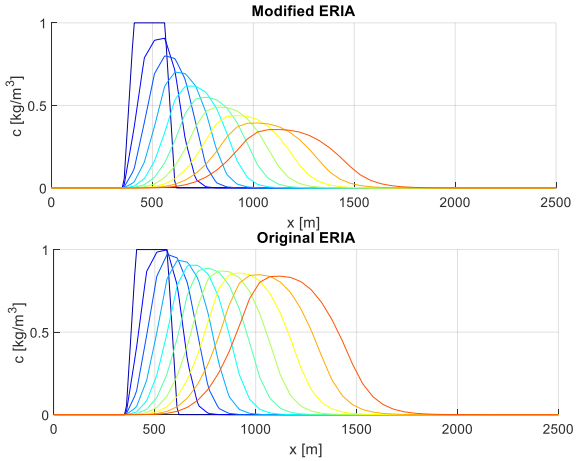

Figure 3 – Temporal variation of suspended sediment concentration along the channel for the modified ERIA scheme (upper figure) and the original ERIA scheme (lower figure).

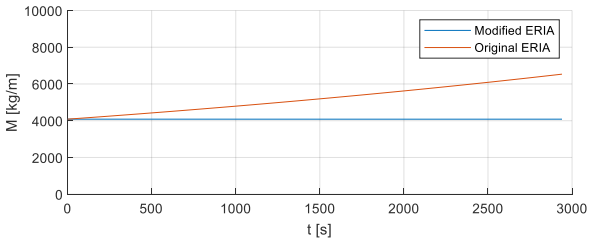

Figure 4 – Temporal variation of the sediment mass for the original ERIA advection scheme (red solid line) and the modified ERIA scheme (blue solid line).

III. APPLICATION: BAR EVOLUTION OVER A SLOPED BEACH IN A LABORATORY EXPERIMENT

A. *Model bathymetry and mesh*

The above improvements have been applied in one of the CROSSTEX experiments [20]. The experiments took place on a wave flume 104 m long, 3.7 m wide and 4.6 m deep. A bar formation has been placed on a 1:20 sloped beach as shown in Figure 5.

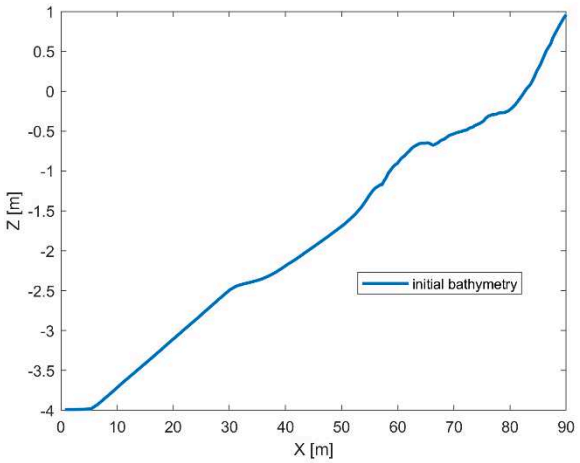

Figure 5 – Initial bathymetry for the CROSSTEX experiments under investigation [20].

An erosive event was studied. This event is generated under wave conditions of TMA spectrum with $H_s = 0.60$ m, $T_p = 4$ s and $\gamma = 2$. In this event the bar migrates from $x = 64$ m to 61 m. The experiment consisted of 14 sets of 15 minutes runs (hence a total time of 3.5 hours).

The numerical domain of length equal to 90 m has been considered according to Figure 5. The mesh resolution was set to 0.2 m, using a channel mesh with a width of three grid nodes, in order to have a quasi one-dimensional setting similar to the laboratory case. The sediment diameter is equal to $d_{50} = 0.2$ mm.

For the TELEMAC-2D simulation a timestep of 1 s was used. The advection scheme considered for tracers was the modified NERD scheme. The Nikuradse bottom friction with constant equal to 0.02 m was used. In TOMAWAC, only advection, shoaling and depth-induced wave breaking, were applied using the new numerical schemes developed in [25]. Monodirectional waves are applied at the boundary. The coupling period with TOMAWAC was set to 300. For GAIA, the Soulsby & van Rijn suspension transport formula has been considered for all sands. The sediment slide has been activated with a friction angle for sediment equal to 30°. The beta parameter for the slope effects, and the cross-shore skewness and asymmetry factors have been calibrated in order to verify the values that give the best results. It has been concluded that beta equal to 0, cross-shore skewness factor equal to 0.3 and cross-shore asymmetry factor equal to 0.1 give the best results that are shown in Figure 6.

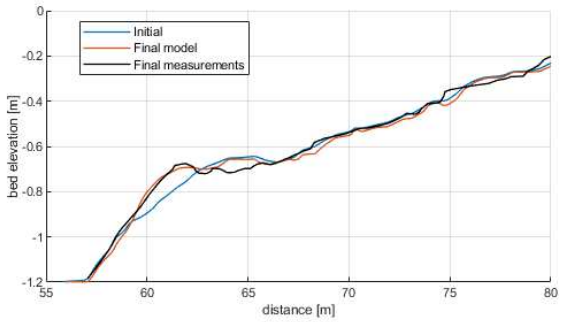

Figure 6 – Initial (blue solid line) and final (red solid line) simulated beach profile and comparison with CROSSTEX experiment under investigation [20] (black solid line).

The resulting beach profile shown in Figure 6. The current development manages to reproduce the migration of the bar to the offshore remarkably similar as observed in the experiment. Nevertheless, there is an area around $x = 63$ m to 66 m from which the results of the model do not show the erosion that occurred in the experiment. This can indicate that the occurring erosion resulting in the bar formation occurs in a much wider area instead of the immediate vicinity of the bar in the initial bathymetry.

In addition, the sediment mass throughout the simulation is shown in Figure 7. The sediment mass difference between the start and the end of the simulation is in total equal to 0.3 kg. This indicates that using the previously described numerical schemes a good conservation of mass is achieved, as the observed error of 0.3 kg is considered sufficiently small, not to have any influence in practical computations. Nevertheless, more research seems desirable to identify the cause of this small mass balance error.

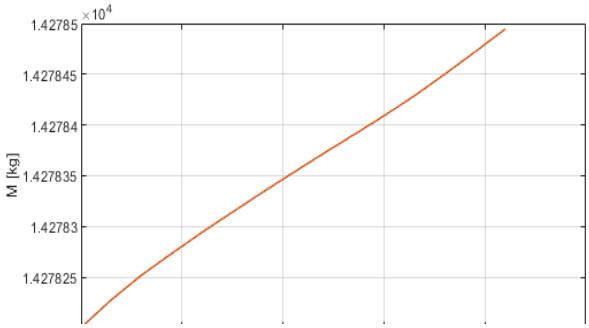

Figure 7 – Temporal variation of the total sediment mass (in suspension and in the bed) for the numerical simulation.

IV. CONCLUSIONS

This paper presents implementations within GAIA module to account for cross-shore sediment transport processes in the nearshore. The mechanisms taken into account include Return flow, Stokes drift, bed slope effects, and non-linear wave effects. The implementations were based on the processes currently implemented in XBeach for cross-shore sediment transport processes. A modified advection scheme was implemented, which advects the sediment volume in the water

column, rather than the depth-averaged sediment concentration, and which uses a correction term to compensate for flow fields that are not divergence-free. A first comparison with cross shore sediment transport in a laboratory experiment was performed, showing promising results. However, more testing is needed to further validate the implemented developments.

REFERENCES

[1] B. Castelle, B. G. Ruessink, P. Bonneton, V. Marieu, N. Bruneau and T. D. Price "Coupling mechanisms in double sandbar systems. Part 1: Patterns and physical explanation," Earth Surface Processes and Landforms, 35(4), pp. 476-486, 2010.

[2] B. Grasmeijer, Process-based cross-shore modelling of barred beaches. PhD thesis, pp.251, University of Utrecht, The Netherlands, 2002.

[3] B.G. Ruessink, G. Ramaekers and L.C. van Rijn, "On the parametrization of the free-stream non-linear wave orbital motionin nearshore morphodynamic models," Coastal Engineering, vol. 65, pp. 56-63, July 2012.

[4] B.G. Ruessink, H. Michallet, T. Abreu, F. Sancho, D.A. Van der A, J.J. Van der Werf and P.A. Silva, "Observations of velocities, sand concentrations, and fluxes under velocity-asymetric oscillatory flows," J. Geophys. Res., 116 (C03004), 2011.

[5] B.G. Ruessink and J.H.J. Terwindt, "The behaviour of nearshore bars on the time scale of years: A conceptual model," Mar. Geol., vol. 163, pp. 289–302, 2000.

[6] B.G. Ruessink, Y. Kuriyama, A.J.H.M. Reniers, J.A. Roelvink and D.J.R. Walstra, "Modelling cross-shore sandbar behaviour on the timescale of weeks," J. Geophys. Res., 112 (F03010), 2007.

[7] C. Berni, Processus de mibilisation et de transport de sédiments dans la zone de déferlement. PhD thesis at Laboratoire des Ecoulements Géophysiques et Industriels (LEGI), Grenoble University, 2011. In French.

[8] D.A. Van der A, T. O'Donoghue and J.S. Ribberink, "Sheet flow sand transport processes in oscillatory flow with acceleration skewness," Proceedings Coastal Dynamics '09, World Scientific, Singapore, 2009.

[9] D.C. Conley and R.A. Beach "Cross-shore sediment transport partitioning in the nearshore during a storm event," Journal of Geophysical Research: Oceans, 108(C3), 2003.

[10] D.L. Foster, A.J. Bowen, R.A. Holman and P. Natoo, "Field evidence of pressure gradient induced incipient motion," Journal of Geophysical Research, 111 (C05004), 2006.

[11] G. Kolokythas, B. De Maerchalck, L. Wang, E. Fonias and W.A. Breugem, "Scaldis-Coast: An Integrated Numerical Model for the Simulation of the Belgian Coast Morphodynamics," In: Geophysical Research Abstracts (Vol. 21), January 2019.

[12] J.A. Roelvink, A. Reniers, A. van Dongeren, J. van Thiel de Vries, R. McCall and J. Lescinski, "Modelling storm impacts on beaches, dunes and barrier islands," Coastal Engineering, 56(11-12), pp. 1133-1152, 2009.

[13] J. Groeneweg. Wave-current interactions in a generalized Lagrangian mean formulation. PhD Thesis, Delft University of Technology, 1999.

[14] J. Jung and Y.-K. Cho, "Persistence of coastal upwelling after a plunge in upwellingfavourable wind," Scientific reports, 10(1), pp. 1-9, Nature Scientific Group, 2020.

[15] J.S.M Van Thiel de Vries, M.R.A. van Gent, D.J.R. Walstra and A.J.H.M. Reniers, "Analysis of dune erosion processes in large-scale flume experiments," Coastal Engineering 55, pp. 1028-1040, 2008.

[16] L. van Rijn and D. Walstra, "Modelling of sand transport in Delft3D," WL | Delft Hydraulics, project Z3624, 2003.

[17] M.S. Longuet-Higgins, "Mass transport in water waves," Phil. Trans. R. Soc., Ser. A 245(03), pp. 535-581, London, 1953.

[18] N. Zimmermann, K. Trouw, B. De Maerschalck, F. Toro, R. Delgado, T. Werwaest and F. Mostaert, "Scientific report regarding hydrodynamics and sand transport in the coastal zone: Evaluation of XBeach for long-term cross-shore modelling," Version 3.0. WL Rapporten, 00_072. Flanders Hydraulics Research & IMDC. Antwerp. Belgium, 2015.

[19] O.M. Phillips, The dynamics of the upper ocean. Cambridge University Press, 1977, pp.366.

[20] P. T. Cobo, J. T. Kirby, M. C. Haller, H. T. Ozkan-Haller, J. Magallen and G. Guannel,. "Model simulations of bar evolution in a large scale laboratory beach, " In Coastal Engineering 2006: (In 5 Volumes), pp.2566-2578, 2007.

[21] R. Soulsby, Overview of Coast3D project. Coast3D project, Paper A1, HR Wallingford Ltd, 2003.

[22] R. Soulsby, Dynamics of marine sands. H.R. Wallingford, 1997.

[23] USACE Coastal Engineering Manual, Chap. III-3-2-a, 2008.

[24] W.A. Breugem, "Ongoing developments in TELEMAC and TOMAWAC in IMDC," XXVIth TELEMAC-MASCARET User Conference, Antwerp, 14-16 October 2020 (submitted).

[25] W.A. Breugem, E. Fonias, L. Wang, A. Bolle, G. Kolokythas and B. De Maerschalck, "TEL2TOM: coupling TELEMAC2D and TOMAWAC on arbitrary meshes," XXVth TELEMAC-MASCARET User Conference, Toulouse, 15-17 October 2019.

[26] WA Breugem, S. Doorme, A. Bakhtiari, J. Figard, and E. Di Lauro, Speeding up TOMAWAC by means of improved numerical methods, submitted to TELEMAC USER CONFERENCE , 2021.